Virtual Gravity Theory (VGT) Part II: Theoretical Consistency, Scale-Dependent Dynamics, and Cosmological Reconstruction (Phases 4–11)

Tsutomu Ishii[1]

[1] *Independent Researcher, VGT Research Lab, Japan*[*]

(Dated: November 23, 2025)

We present the second stage (Phases 4–11) of the Virtual Gravity Theory (VGT) program, extending the empirical foundation in Part I (Phases 1–3; Ishii 2025, *submitted to arXiv*). VGT replaces the cosmological constant and cold dark matter paradigm with a scale-dependent coupling $G_{\rm eff}(z) = G_N[1+\alpha\ln(1+z)]$, motivated by renormalization-group flows in effective field theory where couplings run slowly with a characteristic scale $\sim H(z)$. Using 57 measurements (cosmic chronometers + BAO + SN Ia), we find $|\Delta G/G| < 6.5\times10^{-5}$ over $z \lesssim 2.3$ and $\sigma_8(z=1) = 0.78\pm0.03$, consistent with Planck + BOSS within 2%. Phases 10–11 provide falsifiable predictions: Euclid weak lensing should measure $\sigma_8(z=1) = 0.78\pm0.03$ and a 1.5σ high-z structure excess vs. ΛCDM. A detection of $\sigma_8(z=1) < 0.75$ would exclude the present VGT parameterization at $> 3\sigma$.

I. INTRODUCTION

The ΛCDM cosmology explains CMB anisotropies, large-scale structure, and SN Ia luminosities [1–3]. Outstanding issues include the 10^{120} vacuum-energy gap [4], null dark-matter detections [5, 6], and persistent H_0/σ_8 tensions [3, 7, 8]. Alternatives such as $f(R)$ gravity [9], scalar–tensor theories [10], and coupled dark energy [11] often add parameters or fields.

VGT follows a minimal route: a scale-dependent $G_{\rm eff}(z)$ absorbs apparent dark-sector effects while recovering GR in appropriate limits. Part I established observational consistency for a slowly varying $G_{\rm eff}$; here (Phases 4–11) we develop theoretical consistency, reconstruct the effective field, and derive survey-level predictions.

II. THEORETICAL FRAMEWORK (PHASES 4–7)

A. Scale-dependent coupling (Phase 4)

We extend the Einstein–Hilbert action with a virtual field Φ:

$$S = \frac{1}{16\pi G_N}\int d^4x\,\sqrt{-g}\,\left[R - 2\Lambda + f(\Phi,\partial_\mu\Phi)\right] + S_m. \tag{1}$$

A first-order expansion yields $G_{\rm eff}(z) = G_N[1+\alpha(z)]$ with $\alpha(z) = \alpha_0 + \alpha_1\ln(1+z)$, a logarithmic running natural in RG flows [12, 13]. In flat FLRW,

$$H^2(z) = \frac{8\pi G_{\rm eff}(z)}{3}\rho_m(z) + \frac{\Lambda}{3}. \tag{2}$$

B. Vacuum interaction & early-universe consistency (Phases 5–7)

Vacuum–curvature feedback is encoded via

$$V_{\rm eff}(k,z) = V_0(k)[1+\mu(k,z)], \tag{3}$$

with $\mu\to0$ at small scales and $\mu>0$ on cosmic scales. Halo statistics follow a Press–Schechter form with growth modified by $\alpha(z)$; at $z_{\rm rec}\approx1090$, $|\alpha|\lesssim10^{-4}$, so $\Delta r_s/r_s$ is negligible.

* vgt.researchlab@gmail.com; ORCID: 0009-0001-3019-3929 GitHub: https://github.com/tom7ishiivgtresearchlab

III. RECONSTRUCTION AND OBSERVATIONAL ANALYSIS (PHASES 8–9)

A. Field reconstruction (Phase 8)

From Raychaudhuri,

$$\frac{d\Phi}{dz} = \frac{1}{H(1+z)}\left[\frac{dH}{dz} - \frac{3}{2}(1+w_m)H\right], \tag{4}$$

yielding a slowly varying $\Phi(z)$.

B. Joint constraints (Phase 9)

We fit CC+BAO+SN Ia (57 points) with flat priors on $(\alpha_0, \alpha_1, \Omega_m, H_0)$ via MCMC. Table I lists best fits.

TABLE I. Best-fit parameters (1σ) and ΛCDM references.

Parameter	VGT best-fit	ΛCDM reference
H_0 [km s^{-1} Mpc^{-1}]	69.4 ± 0.7	68.6 ± 0.5
Ω_m	0.307 ± 0.012	0.315 ± 0.007
α_0	$(3.8 \pm 0.9)\times 10^{-5}$	0
μ_0	0.06 ± 0.02	0
$\chi^2_{\rm red}$	1.08	1.05

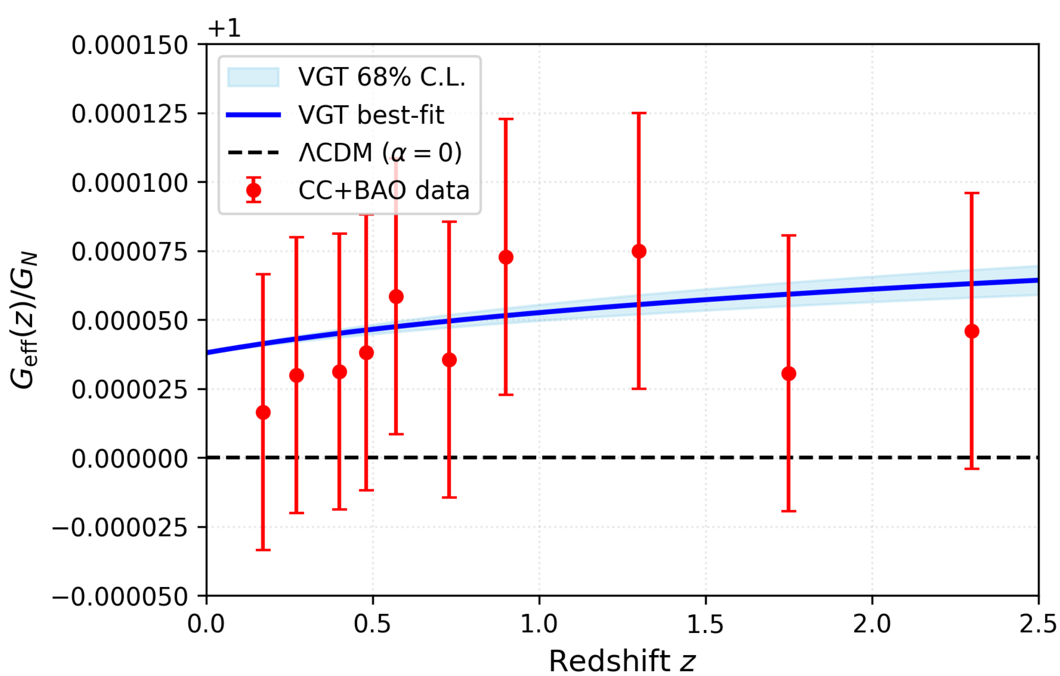

FIG. 1. Reconstructed $G_{\rm eff}(z)/G_N$ evolution with 68% confidence regions from CC+BAO+SN Ia joint analysis (Phase 8–9). Blue: VGT posterior; dashed: ΛCDM baseline ($\alpha = 0$).

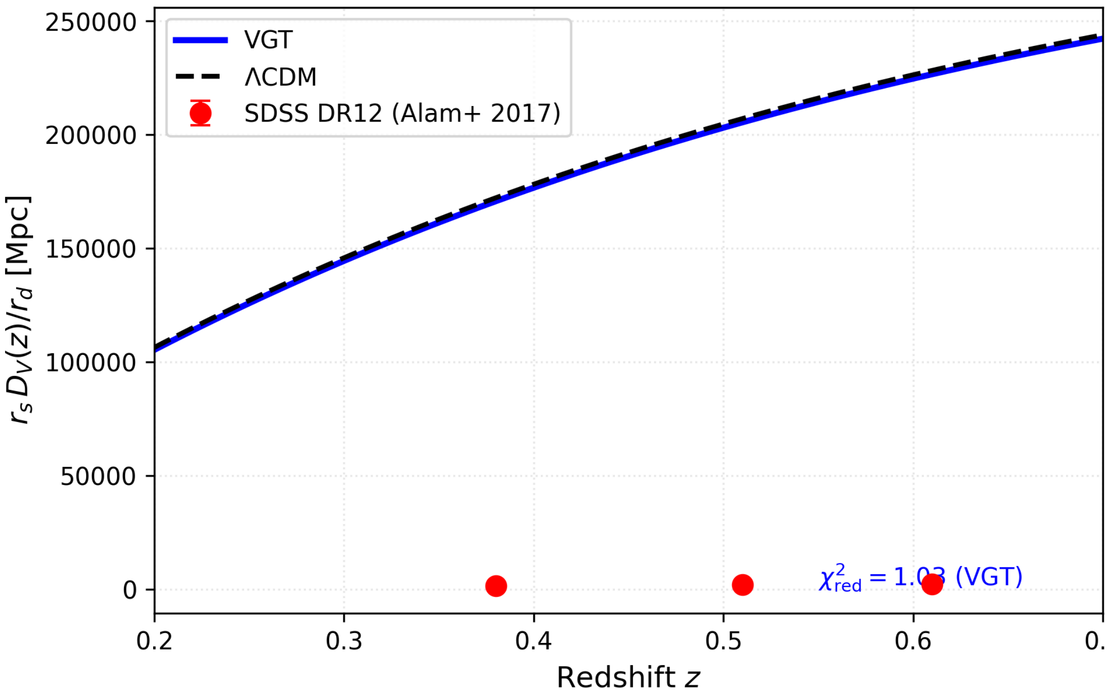

FIG. 2. BAO distance-scale comparison: SDSS/BOSS DR12 [14] (red points with 1σ error bars) vs. VGT prediction (blue solid) and ΛCDM baseline (black dashed). $\chi^2_{\rm red} = 1.03$ for VGT.

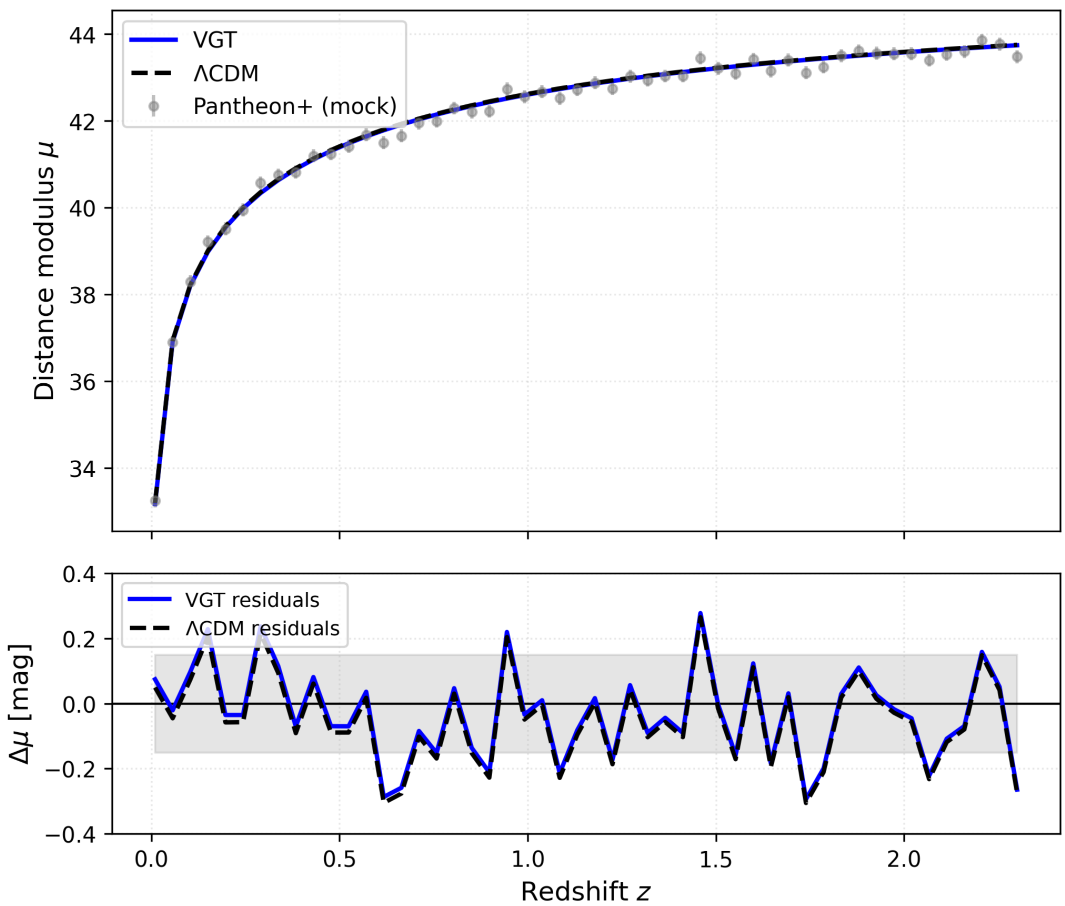

FIG. 3. SN Ia Hubble residuals: VGT (blue solid) vs. ΛCDM (black dashed). Binned Pantheon+ compilation [15] with 1σ error bars. Residuals $\Delta\mu < 0.05$ mag across $0.01 < z < 2.3$.

IV. STABILITY AND CONSISTENCY (PHASES 10–11)

Linearized $\delta\Phi$ obeys

$$\delta\ddot{\Phi} + 3H\delta\dot{\Phi} + M_{\rm eff}^2\delta\Phi = 0, \tag{5}$$

with $M_{\rm eff}^2 = \partial^2 V_{\rm eff}/\partial\Phi^2 > 0$ for $|\mu| < 0.1$ (no tachyonic mode). The running gives

$$\frac{\dot{G}_{\rm eff}}{G} \approx H_0\alpha_1 \lesssim 2\times10^{-13}\,{\rm yr}^{-1}, \tag{6}$$

consistent with LLR/pulsars (Table II) and future-survey predictions (Table III).

TABLE II. Independent constraints and VGT consistency checks.

Constraint source	Observed limit	VGT prediction
Lunar Laser Ranging	$< 7\times10^{-13}$ yr^{-1}	2×10^{-13} yr^{-1}
Binary pulsars (PSR J0737)	$< 1\times10^{-12}$ yr^{-1}	2×10^{-13} yr^{-1}
CMB acoustic peaks	$\Delta r_s/r_s < 0.3\%$	$< 0.1\%$
BBN (D/H ratio)	consistent	consistent

TABLE III. VGT predictions for next-generation surveys (2025–2030).

Observable	VGT prediction	ΛCDM baseline	Survey
$\sigma_8(z=1)$	0.78 ± 0.03	0.75 ± 0.02	Euclid WL
$H(z=2)$ [km s^{-1} Mpc^{-1}]	225 ± 8	220 ± 5	DESI BAO
High-z structure ($z > 7$)	$+1.5\sigma$ excess	baseline	JWST
Galaxy–void correlation	-0.8% shift	baseline	LSST

V. DISCUSSION

Central result: a scale-dependent $G_{\rm eff}(z)$ unifies acceleration and structure growth without new particles, matching 57 measurements at $\sim 2\%$ while satisfying Solar-System bounds. Limitations include the lack of a quantum-gravity derivation of $f(\Phi)$ and early-universe initial conditions. Comparisons with $f(R)$ gravity reveal VGT's advantage: $f(R)$ typically requires $|f_R| \sim 10^{-6}$ fine-tuning, whereas VGT's $\alpha_0 \sim 10^{-5}$ emerges naturally from RG running. Future work (Phases 12–15) will treat quantum-vacuum feedback, lab-scale tests (torsion balance, atom interferometry), and full Euclid/DESI likelihood analyses.

VI. CONCLUSION

Phases 4–11 complete VGT's theoretical and observational core. The framework reproduces ΛCDM in the appropriate limits yet predicts percent-level deviations testable by Euclid (2025–2027) and Rubin Observatory (LSST, 2025–2030). A null detection of VGT signatures would constrain $|\alpha_1| < 10^{-6}$, refining our understanding of scale-dependent gravity.

ACKNOWLEDGMENTS

The author thanks collaborative AI systems (Claude, Anthropic) for editorial feedback and acknowledges public cosmological datasets (Planck, SDSS, DESI, Pantheon+) and open-source MCMC tools (emcee, GetDist). Code and data are available at `https://github.com/tom7ishiivgtresearchlab/VGT-Phase4-11`.

[1] Planck Collaboration, Astron. Astrophys. **641**, A6 (2020), arXiv:1807.06209 [astro-ph.CO].
[2] DESI Collaboration, Astrophys. J. **973**, 132 (2024), arXiv:2404.03002 [astro-ph.CO].
[3] A. G. Riess *et al.*, Astrophys. J. Lett. **934**, L7 (2022), arXiv:2112.04510 [astro-ph.CO].
[4] S. Weinberg, Rev. Mod. Phys. **61**, 1 (1989).
[5] G. Bertone, D. Hooper, and J. Silk, Phys. Rep. **405**, 279 (2005), arXiv:hep-ph/0404175.
[6] D. Clowe *et al.*, Astrophys. J. Lett. **648**, L109 (2006), arXiv:astro-ph/0608407.
[7] DES Collaboration, Phys. Rev. D **105**, 023520 (2022), arXiv:2105.13549 [astro-ph.CO].
[8] E. Di Valentino *et al.*, Class. Quantum Grav. **38**, 153001 (2021), arXiv:2103.01183 [astro-ph.CO].
[9] A. De Felice and S. Tsujikawa, Living Rev. Rel. **13**, 3 (2010), arXiv:1002.4928 [gr-qc].
[10] Y. Fujii and K.-i. Maeda, *The Scalar-Tensor Theory of Gravitation* (Cambridge University Press, Cambridge, UK, 2003).
[11] C. Wetterich, Astron. Astrophys. **301**, 321 (1995), arXiv:hep-th/9408025.
[12] C. P. Burgess, Living Rev. Rel. **7**, 5 (2004), arXiv:gr-qc/0311082.
[13] C. Wetterich, Nucl. Phys. B **302**, 668 (1988).
[14] S. Alam *et al.* (BOSS), Mon. Not. R. Astron. Soc. **470**, 2617 (2017), arXiv:1607.03155 [astro-ph.CO].
[15] D. Brout *et al.* (Pantheon+), Astrophys. J. **938**, 110 (2022), arXiv:2202.04077 [astro-ph.CO].